Journal of Environmental Management 245 (2019) 230–237

Contents lists available at ScienceDirect

Journal of Environmental Management

journal homepage: www.elsevier.com/locate/jenvman

Research article

An imperative approach for fluorosis mitigation: Amending aqueous calcium to suppress hydroxyapatite dissolution in defluoridation

Ravi Sankannavar[a,b,*], Sanjeev Chaudhari[a]

[a] Centre for Environmental Science and Engineering, Indian Institute of Technology Bombay, Powai, Mumbai, 400 076, India
[b] Department of Chemical Engineering, Indian Institute of Technology Bombay, Powai, Mumbai, 400 076, India

ARTICLE INFO

Keywords:
Drinking water
Fluoride removal
Hydroxyapatite dissolution
Phosphate leaching
Calcium amendment
Fluorosis reversal

ABSTRACT

Drinking of fluoride (F^-) contaminated water causes fluorosis and thus providing safe drinking water to the affected community remains a major challenge. Therefore, defluoridation without disturbing water quality is imperative. Hydroxyapatite (HAP) is proved to have a potential application for defluoridation; however, its dissolution during defluoridation is a concern for its implementation. Experiments conducted by suspending HAP in F^- solution and deionized water without F^- show that former had high residual pH and PO_4^{3-} than the latter with Ca^{2+} being absent in the former. This indicates that Ca^{2+} had participated in defluoridation and promoted HAP dissolution when Ca^{2+} was unavailable. Hence, HAP dissolution seems to be a governing step for defluoridation. However, higher residual PO_4^{3-} and pH affect drinking water quality, and its usage may pose additional health problems. Thus, Ca^{2+} deficient defluoridated water is unfit for drinking unless it is treated further. Hence, the present work proposes a novel method to overcome HAP dissolution by amending aqueous Ca^{2+} to F^- water. The results show that amending Ca^{2+} efficiently prevents HAP dissolution and enhances defluoridation capacity as an added feature. Furthermore, speciation using MINEQL+ and FTIR of fluoride-calcium treated HAPs suggest the possibility of defluoridation by aqueous CaF^+ adsorption onto HAP besides F^- ion exchange with OH^-.

1. Introduction

Groundwater is one of the primary sources of water for many regions of the world for our daily needs as it is fresh and generally of good microbial quality than surface water (Schmoll et al., 2006). However, due to the geological contamination, the higher level of fluoride (F^-) in groundwater has been a major cause of concern for its utilization (Brindha et al., 2011; Patel et al., 2014; Rafique et al., 2015). Around 200 million people from 25 nations in the world, including most populated countries like China and India, and a significant population from Eastern Africa are worst affected by the presence of excess F^- in their drinking water (Susheela, 2002; Ayoob et al., 2008). The F^- presence in drinking water is providing divergent health effects on consumers depending on the amount of F^- ingested (Whelton et al., 2004; Fawell et al., 2006). In a brief, consumption of water containing 0.5 mg F^-/L found to be beneficial in reducing dental decay. But, exposure to excess $F^- > 1$–1.5 mg F^-/L causes a group of diseases called as "fluorosis," primarily consisting of dental and skeletal fluorosis. However, Susheela (2002) and MacDonald et al. (2011) reported the appearance of fluorosis even below the desirable limit of 1 mg F^-/L prescribed by the Bureau of Indian Standards (2012). Hence, Susheela (1999, 2002, 2007) proposes the revision of the guideline value for F^- is required and suggested to avoid consumption of F^- contaminated water and food.

Considerable research has been done on fluoride removal or defluoridation to provide potable drinking water to fluorosis affected areas (Meenakshi and Maheshwari, 2006; Ayoob et al., 2008; Mohapatra et al., 2009; Bhatnagar et al., 2011; Izuagie et al., 2016). Several defluoridation methods have been suggested in the past; however, Nalgonda technique, use of activated alumina, and reverse osmosis are most commonly employed methods. Even though these methods can successfully remove F^- well below 1 mg F^-/L, the problem of fluorosis persists (Meenakshi and Maheshwari, 2006; Ayoob et al., 2008), which is due to their inability to successfully implement these methods in the fluorosis affected areas (Yadugiri, 2011). The possible demerits of these defluoridation methods briefly are as follows. The Nalgonda technique requires careful monitoring of alkalinity, and residual Al^{3+} and SO_4^{2-} concentrations as these parameters may exceed the desirable limits (Meenakshi and Maheshwari, 2006). Defluoridated water using activated alumina exceeds the desirable limit for residual

---

[*] Corresponding author. Department of Chemical Engineering, Indian Institute of Technology Bombay, Powai, Mumbai, 400 076, India.
E-mail address: ravi.sankannavar@gmail.com (R. Sankannavar).

https://doi.org/10.1016/j.jenvman.2019.05.088
Received 29 November 2017; Received in revised form 11 January 2019; Accepted 21 May 2019
0301-4797/

Al^{3+}, and requires periodic regeneration of saturated alumina and environmentally acceptable disposal process for exhausted alumina (Shreyas et al., 2013). Whereas reverse osmosis requires electricity and pre-treatment of feed to avoid fouling of membrane, and reject water disposal becomes another issue (Ayoob et al., 2008; Anjaneyulu et al., 2012; Samrat et al., 2018). Nevertheless, use of these defluoridation methods will not resolve the problem of safe drinking water unless combining with an additional treatment method (Anjaneyulu et al., 2012; Samrat et al., 2018). Even though some of the defluoridation methods were implemented in the fields; the number of fluorosis affected cases is increasing although the fluorosis problem is quite old (Ayoob et al., 2008). Hence, health problems may continue to grow if the issue of F^- contamination in drinking water persists.

To overcome demerits of most commonly used defluoridation methods and resolve the problem of safe drinking water, researchers used synthetic (Fan et al., 2003; Sundaram et al., 2008; Nie et al., 2012; Sani et al., 2016) and natural, in the form of bone char (Medellin-Castillo et al., 2016; Delgadillo-Velasco et al., 2017), hydroxyapatite (HAP or $Ca_{10}(PO_4)_6(OH)_2$) as a defluoridation media. The HAP is considered as a potential material for defluoridation due to its selective propensity to uptake F^- and higher defluoridation capacity (He and Cao, 1996; Fan et al., 2003). However, use of bone char for water treatment may not be universally accepted due to religious beliefs, and microbiological and aesthetic problems (Fawell et al., 2006). Therefore, use of HAP synthesized using locally available and inexpensive raw materials (MacDonald et al., 2011; Yakub and Soboyejo, 2013; Kanno et al., 2014) is preferable over bone char. In order to examine its feasibility for defluoridation, few of the previous laboratory studies (He and Cao, 1996; Lessard, 2007; Sternitzke et al., 2012; Kanno et al., 2014) reported HAP dissolution during the defluoridation. However, dissolution of HAP leaches calcium (Ca^{2+}) and phosphate (PO_4^{3-}) ions and increases the pH of water, which negatively affects the water quality, particularly when residual PO_4^{3-} is present in excess.

Presently, no Bureau of Indian Standards for PO_4^{3-} in drinking water exist. However, some of the recent studies reported toxicity of PO_4^{3-} and its adverse health effects on human (Razzaque, 2011; Ritz et al., 2012; Jain and Elsayed, 2013; Brown and Razzaque, 2015; Anukam and Agu, 2017). It has been reported that impaired balance of PO_4^{3-} affects musculoskeletal and cardiovascular systems, excess intake of PO_4^{3-} leads to an increase in mortality and morbidity, accelerates ageing process, and causes hyperphosphatemia, which further promotes the hypocalcemia. A survey by the National Health and Nutrition Education (2005–2006) reported that estimated PO_4^{3-} intake exceeded the estimated average requirement in adults (Moshfegh et al., 2009). The phosphorus present in the food mostly exists as organic phosphate with bound form, whereas in drinking water, it is in orthophosphate (inorganic) form. Thus, intestinal absorption of artificial inorganic phosphate present in the drinking water is much more than the natural phosphate present in the food (Anukam and Agu, 2017). Moreover, the absorption of PO_4^{3-} in the intestine is twice of that of Ca^{2+} ions (Razzaque, 2011). Further, the PO_4^{3-} present in drinking water reduces the bioavailability of Ca^{2+} and Mg^{2+} ions present in the diet and water by forming insoluble salts (Guéguen and Pointillart, 2000; Prasad and Bhadauria, 2013), which poses an additional problem of cation minerals deficiency. It is also vital to note that the presence of Ca^{2+} or Mg^{2+} ions helps in decreasing the bioavailability of F^- (Heard et al., 2001). Hence, any reduction in the bioavailability of these divalent cations due to the presence of PO_4^{3-} in water further increases the chances of F^- absorption into the gastrointestinal tract. Thus, individuals drinking water containing both F^- and PO_4^{3-} ions might have a negative impact on their health.

Besides PO_4^{3-} toxicity, the HAP dissolution during the defluoridation gradually reduces the quantity of HAP. Hence, HAP dissolution is a primary concern in the defluoridation. Thus, identifying the cause of HAP dissolution during the defluoridation facilitates the efficient use of HAP to provide safe drinking water. Hence, in the present work, an effort has been made to prevent HAP dissolution to achieve safe drinking water. A recent study reported that the addition of F^- to HAP suspension containing Ca^{2+} and PO_4^{3-} ions reduced Ca^{2+} concentration (Sternitzke et al., 2012). Another study observed that defluoridation did not take place in the absence of bone char (natural HAP) even though solution containing Ca^{2+} and F^- ions was supersaturated with respect to fluorite (Jacobsen and Dahi, 1997). Moreover, the addition of Ca^{2+} salt to F^- water enhanced the defluoridation capacity of bone char (Jacobsen and Dahi, 1997) and residual Ca^{2+} in the HAP suspension decreased only in the presence of F^- (Sternitzke et al., 2012). Thus, by above adduced facts, we hypothesize that aqueous Ca^{2+} has a role when we use HAP for defluoridation. Therefore, herein, we have conducted defluoridation experiments by amending aqueous Ca^{2+} to F^- water before contact with uncalcined HAP. The outcome from the present study provides the synergistic effect of HAP and aqueous Ca^{2+} for efficient defluoridation without changing the quality of drinking water. Further, we have discussed possible mechanisms of defluoridation using HAP for a case when amended Ca^{2+} has a role in the process of defluoridation.

2. Materials and methods

2.1. Synthesis of uncalcined hydroxyapatite

In this study, HAP was synthesized by the wet chemical precipitation method at room temperature (27 °C). Briefly, diammonium hydrogen phosphate ($(NH_4)_2HPO_4$) solution was slowly added to the $Ca(OH)_2$ suspension with continuous stirring at 500 rpm. After complete mixing of both solutions, the suspension was additionally stirred for 10 min at 600–700 rpm. The final concentrations of Ca^{2+} and PO_4^{3-} ions in the mixture were 777.5 and 465.6 mM, respectively for an ideal Ca/P molar ratio of 1.67. Additionally, the precipitate was allowed to stand with the mother solution for 3 h, and then separated the supernatant by centrifuging at 3300 G-force for 5 min. Further, the precipitate was washed twice using deionized water followed by centrifugation. This wet HAP paste was dried at 80 °C for overnight using hot air oven. Further, the dried HAP was ground to a powder using porcelain mortar and pestle. This uncalcined HAP powder was ground to pass a 45-mesh (355 μm) sieve but retained on a 500-mesh sieve (25 μm).

The material characterization of an uncalcined HAP was carried out by the Fourier transform infrared (FTIR), X-ray diffraction (XRD) and high-resolution transmission electron microscopy (HRTEM) with energy dispersive spectroscopy (EDS), and these details are provided in the Supplementary material S1.2. The experimental details for the measurement of the actual Ca/P molar ratio and the specific surface area of the HAPs are also provided in the Supplementary material S1.3.

2.2. Defluoridation experiments using hydroxyapatite

The defluoridation experiments were conducted at room temperature (29 ± 1 °C) as follows. Accurately weighed 100 mg of HAP powder was suspended in 100 mL of 10 mg F^-/L solution. However, the pH of the F^- solution was adjusted to pH 7 using 0.1 M NaOH solution before suspending HAP into the solution. After suspending HAP into the F^- solution, the bottles were tightly closed and then rotated using the end-over-end rotor with 60 ± 1 rpm. At the predetermined time intervals from 1 to 24 h, HAP was separated from F^- solution by filtration using glass microfiber filter papers (GF/C, 1.2 μm). The F^- treated HAPs collected on filter papers were dried at room temperature. Similar experiments were also conducted by suspending HAP in deionized water; but without addition of F^-, which help in assessing a role of F^- on HAP dissolution. The pH and concentrations of F^-, Ca^{2+} and PO_4^{3-} ions were measured before and after contact with HAP. The details of chemical analysis methods adopted for the measurement of F^-, Ca^{2+} and PO_4^{3-} ion concentrations are provided in the Supplementary material S1.4. All these experiments were conducted in triplicate.

2.3. Defluoridation using hydroxyapatite and amending aqueous calcium to fluoride water

Beside the defluoridation and without F^- experiments, additional defluoridation kinetic experiments were also conducted by amending aqueous Ca^{2+} to F^- water. However, the Ca^{2+} was amended to the F^- solution before suspending HAP into the solution. In these experiments, aqueous Ca^{2+} was amended to the F^- solution (10 mg F^-/L) in two ranges of Ca^{2+} concentrations, 1–7 mg Ca^{2+}/L (low calcium amendment) and 10–40 mg Ca^{2+}/L (high calcium amendment). These aqueous calcium amended defluoridation experiments were conducted using the procedure described in subsection 2.2 to examine the effect Ca^{2+} amendment on the dissolution of HAP. Further, the fluoride-calcium (F–Ca) treated HAPs were separated from the solution for further chemical analysis and characterization of treated HAPs. The chemical speciation and saturation indices (SIs) calculations were done using MINEQL+ (Version 4.5) chemical equilibrium modeling system (Schecher and McAvoy, 1992) and the details are provided in subsection S1.5 of the Supplementary material.

3. Results and discussion

3.1. Characterization of synthesized uncalcined hydroxyapatite

The presence of PO_4^{3-} and OH^- groups were confirmed from the FTIR (Fig. S1a), whereas the HAP phase formation was confirmed from the XRD (Fig. S1b). Hence, FTIR and XRD characterizations suggest that the uncalcined synthesized powder was HAP. The TEM image of the untreated HAP (Fig. S2a) shows that HAP particles are rod-like shape. The details of these characterization techniques are provided in the Supplementary material S2.1.

3.2. An actual Ca/P molar ratio and BET specific surface area of hydroxyapatite

The measured actual Ca/P molar ratio of HAP was found to be 1.61 ± 0.05. This measured ratio is comparable with the literature value of 1.60 for HAP, which was prepared using $Ca(OH)_2$ and H_3PO_4 raw materials (Smičiklas et al., 2006). The actual Ca/P ratios are less than the stoichiometric ratio of an ideal HAP, i.e., 1.67, which suggests that the prepared HAPs were deficient in calcium. The measured BET specific surface area of uncalcined HAP was 92.69 ± 0.06 m^2/g, which is 2.2 times higher than that of the calcined HAP (42.09 ± 0.05 m^2/g) at 700 °C for 3 h. A similar trend in the reduction of the BET surface area of HAP after calcination was also observed and found be an uncalcined HAP had higher adsorption capacity (Bahdod et al., 2009). Thus, in this study an uncalcined HAP was used for defluoridation to utilize the maximum surface area. Henceforth, the numbers before and after plus-or-minus signs represent the average values of three replicates and the 95% confidence limits, respectively.

3.3. Defluoridation experiments without amending aqueous calcium

Defluoridation experiments conducted without amending aqueous Ca^{2+} (F = 10 mg F^-/L, Ca = 0 Ca^{2+}/L) from 1 to 24 h of contact time show that the pH (Fig. 1a) and residual PO_4^{3-} (Fig. 1b) increased with an increase in contact time. However, a very low level of Ca^{2+} was observed only at first instance (1 h), and the Ca^{2+} concentration was below the detection limit of 0.05 mg Ca^{2+}/L for contact time of more than 1 h (Fig. 1c). A similar trend of decrease in the residual Ca^{2+} during the defluoridation was also reported by Lessard (2007) and Sternitzke et al. (2012). Additional experiments conducted without F^- (F = 0 mg F^-/L, Ca = 0 Ca^{2+}/L in Fig. 1c) have higher concentration of Ca^{2+} (1.13 ± 0.04–1.62 ± 0.03 mg Ca^{2+}/L) than that of the defluoridation experiments with the only F^-. However, the values of pH and residual PO_4^{3-} are always higher for defluoridation experiments compared to those without F^- (Fig. 1a and b). It has been also reported that the HAP has higher solubility in the presence of F^- compared to the pure HAP (Aljerf and Choukaife, 2017; Choukaife and Aljerf, 2017). Thus, from these results, it is clear that the presence of F^- probably promoted HAP dissolution. Similar trends of increase in the values of pH (Nie et al., 2012) and residual PO_4^{3-} (Sternitzke et al., 2012) were also reported in the past when Al-HAP and nano-HAP, respectively were used for defluoridation.

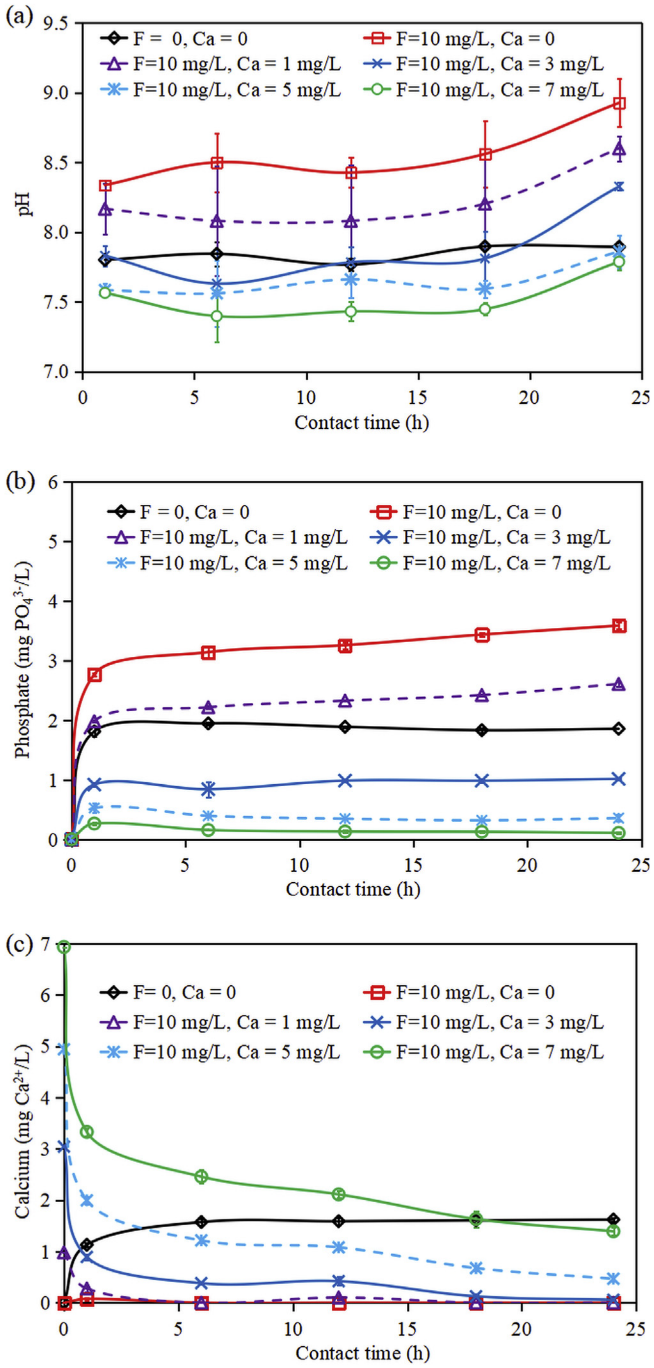

Fig. 1. The effect of low amended aqueous calcium (0–7 mg Ca^{2+}/L) on residual (a) pH, (b) phosphate, and (c) calcium of treated water for 10 mg F^-/L solution and without fluoride solution with initial pH of 7 and 1 g/L of HAP at room temperature (29 ± 1 °C) for contact time from 1 to 24 h. Data points and error bars represent average values of three replicates and the 95% confidence limits, respectively; sometimes error bars are smaller than symbols.

Precipitation of minerals such as HAP, fluorapatite ($Ca_5(PO_4)_3F$ or

FAP) or fluorite (CaF_2), or adsorption of Ca^{2+} ions and/or Ca–F complex onto HAP likely reduce the residual Ca^{2+} during defluoridation. The possibility of minerals precipitation in the solution was evaluated by calculating the SIs using MINEQL + and SIs are presented in Table S2. The SIs were oversaturated ($SI > 0$) with respect to HAP for experiments without F^-, whereas defluoridation experiments were undersaturated ($SI < 0$) with respect to all the minerals considered. Thus, possibly the HAP precipitation occurred in the absence of F^-, whereas precipitation of minerals did not reduce Ca^{2+} in the defluoridation experiments. However, residual Ca^{2+} was decreased (Fig. 1c) even though there was no precipitation of minerals in defluoridation as observed from SIs (Table S2). Hence, it requires an evaluation of the possibility of re-adsorption of Ca^{2+} ions or its complex in the defluoridation experiments, and it is discussed in subsection 3.7 of defluoridation mechanisms.

3.4. *Defluoridation experiments by amending aqueous calcium to the fluoride water*

Results for the further defluoridation experiments conducted with low level calcium amendment (1–7 mg Ca^{2+}/L) to 10 mg F^-/L solution are presented in Fig. 1. From Fig. 1a, amending a very low level of aqueous Ca^{2+} (1 mg Ca^{2+}/L) lowered the increase in the pH from 8.93 ± 0.17 to 8.60 ± 0.09 at 24 h of contact time. Increase in the amended aqueous Ca^{2+} to 7 mg Ca^{2+}/L, further lowered an increase in the pH of defluoridated water to pH 7.79 ± 0.06 (Fig. 1a). Furthermore, increase in amending aqueous Ca^{2+} from 1 to 7 mg Ca^{2+}/L reduced the residual PO_4^{3-} concentration from 2.60 ± 0.04 to 0.11 ± 0.02 mg PO_4^{3-}/L (Fig. 1b). Also, the residual PO_4^{3-} values for aqueous Ca^{2+} amended defluoridation experiments were much lower than that of defluoridation without amended Ca^{2+} (3.58 ± 0.06 mg PO_4^{3-}/L), and without F^- and Ca^{2+} (1.85 ± 0.05 mg PO_4^{3-}/L) experiments. Thus, it was clear that amending aqueous Ca^{2+} suppressed the HAP dissolution, which was increasing the pH and PO_4^{3-} values of defluoridated water. It is worth noting that the residual Ca^{2+} was always lower than the amended Ca^{2+} and it was decreased from 7 to 1.39 ± 0.08 mg Ca^{2+}/L for an increase in contact time from 0 to 24 h (Fig. 1c). In the past, a similar trend for a decrease in the residual Ca^{2+} was also reported but by addition of high amount of F^- (62.7 mg F^-/L) to an equilibrated solution containing 2 g/L HAP (Sternitzke et al., 2012). Thus, the decrease in the concentration of amended aqueous Ca^{2+} supports the requirement of aqueous Ca^{2+} ions for defluoridation of water using HAP.

Additional defluoridation experiments conducted by amending a higher concentration of Ca^{2+} (10–40 mg Ca^{2+}/L) to F^- solution (10 mg F^-/L) showed little effect on lowering the increase in the pH (Table 1). The values of pH of defluoridated water are within the desirable range (pH 6.5–8.5) prescribed by the Bureau of Indian Standards (2012) for all values of amended Ca^{2+} except for 1 mg Ca^{2+}/L at the end of 24 h. The residual PO_4^{3-} is below the detection limit of 0.03 mg PO_4^{3-}/L for defluoridated water when amended Ca^{2+} was 20 mg Ca^{2+}/L or more (Table 1) at 24 h. In conclusion, the absence of PO_4^{3-} in defluoridated water suggests that the use of 20 mg Ca^{2+}/L aqueous calcium efficiently prevented PO_4^{3-} leaching from HAP and an increase in the pH.

3.5. *Particle size analysis and Ca/P atomic ratios of hydroxyapatites*

The particle size analysis was carried out to assess the effect of F^- on HAP's size after defluoridation using TEM images (Fig. S2). The particle size analysis shows that treating of HAP in F^- solution reduces the size of HAP (Table S1), which was due to the dissolution of HAP as noted in subsection 3.3. It is noteworthy to highlight here that the size of F^- treated HAP (F-HAP) is smaller than those of untreated (HAP), treated in deionized water (DI-HAP) and F–Ca treated (F–Ca-HAP) HAPs, which supports the presence of F^- promotes the dissolution of HAP. The order of the particle size of HAPs is as follows: F-HAP < DI-HAP < F–Ca-HAP < HAP. The Ca/P atomic ratios measured using EDS (Table S1) show that F–Ca-HAP has higher ratio than other HAPs. The atomic ratios follow the order: DI-HAP < HAP < F-HAP < F–Ca-HAP. The higher atomic ratios for F–Ca-HAP and F-HAP compared to the untreated HAP were observed, which were due to the adsorption of Ca^{2+} or its complex from the amended aqueous Ca^{2+} and F^- solution for F–Ca-HAP; whereas it is due to the readsorption of Ca^{2+} or its complex from F^- solution and/or leaching of PO_4^{3-} ions from the HAP for F-HAP.

Table 1
The effect of high aqueous calcium (10–40 mg Ca^{2+}/L) on residual values of (i) pH, (ii) calcium, and (iii) phosphate of defluoridated water using hydroxyapatite.

Time (h)	Aqueous calcium amended (mg Ca^{2+}/L)			
	10	20	30	40
(i) pH				
1	7.44 ± 0.14	7.30 ± 0.10	7.19 ± 0.06	7.19 ± 0.03
6	7.45 ± 0.01	7.38 ± 0.05	7.25 ± 0.03	7.22 ± 0.02
12	7.52 ± 0.20	7.36 ± 0.09	7.29 ± 0.08	7.19 ± 0.06
18	7.24 ± 0.10	7.34 ± 0.01	7.23 ± 0.02	7.19 ± 0.05
24	7.35 ± 0.11	7.49 ± 0.03	7.34 ± 0.05	7.28 ± 0.07
(ii) residual calcium (mg Ca^{2+}/L)				
1	5.41 ± 0.03	14.1 ± 0.2	23.0 ± 0.3	32.6 ± 0.1
6	4.08 ± 0.05	12.8 ± 0.1	21.3 ± 0.2	30.7 ± 0.4
12	3.6 ± 0.2	12.0 ± 0.2	20.8 ± 0.2	29.8 ± 0.1
18	3.35 ± 0.06	11.5 ± 0.2	20.28 ± 0.08	29.55 ± 0.05
24	3.15 ± 0.06	11.12 ± 0.08	19.8 ± 0.2	29.2 ± 0.2
(iii) residual phosphate (mg PO_4^{3-}/L)				
1	0.13 ± 0.02	0.05 ± 0.01	< 0.03	< 0.03
6	0.06 ± 0.01	0.05 ± 0.02	< 0.03	< 0.03
12	0.14 ± 0.06	< 0.03	< 0.03	< 0.03
18	0.13 ± 0.03	< 0.03	< 0.03	< 0.03
24	0.10 ± 0.05	< 0.03	< 0.03	< 0.03

3.6. *The effect of amending aqueous calcium on the defluoridation capacity*

In addition to the results of prevention of PO_4^{3-} leaching and pH increase, the effect of amended aqueous Ca^{2+} on defluoridation capacity is also presented in Fig. 2. From Fig. 2, the addition of a small amount of calcium (7 mg Ca^{2+}/L) to F^- water enhanced the defluoridation capacity 1.58 times (i.e., 2.07 mg/g) of that of without amended Ca^{2+} at the end of 24 h contact time. It is also observed that the defluoridation kinetics enhanced as indicated by an increase in the defluoridation capacity from 3.82 ± 0.03 to 5.63 ± 0.03 mg/g when contact time was increased from 1 to 24 h for initial 7 mg Ca^{2+}/L

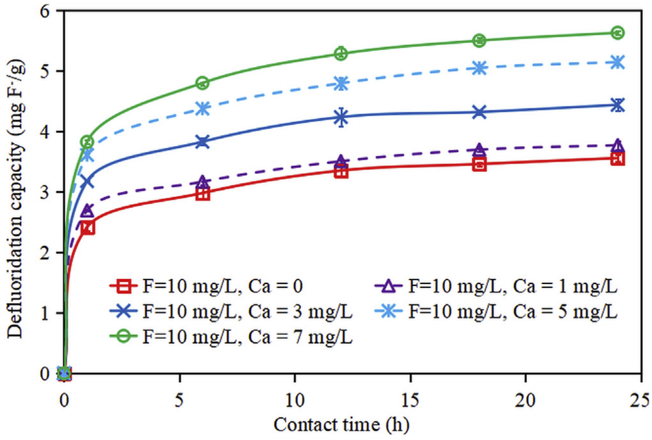

Fig. 2. Effect of low amended aqueous calcium (0–7 mg Ca^{2+}/L) on defluoridation capacity. Data points and error bars represent average values of three replicates and the 95% confidence limits, respectively; sometimes error bars are smaller than symbols.

Table 2
The effect of high amended aqueous calcium (10–40 mg Ca^{2+}/L) on the defluoridation capacity of hydroxyapatite.

Time (h)	Aqueous calcium amended (mg Ca^{2+}/L)			
	10	20	30	40
	Defluoridation capacity (mg F^-/g of HAP)			
1	4.03 ± 0.05	4.75 ± 0.03	4.99 ± 0.03	5.19 ± 0.01
6	5.17 ± 0.03	6.05 ± 0.02	6.42 ± 0.05	6.54 ± 0.02
12	5.7 ± 0.1	6.46 ± 0.02	6.76 ± 0.02	6.99 ± 0.05
18	5.99 ± 0.03	6.76 ± 0.04	7.20 ± 0.07	7.34 ± 0.03
24	6.21 ± 0.05	6.94 ± 0.04	7.34 ± 0.07	7.48 ± 0.02

solution. A previous study by Jacobsen and Dahi (1997) also reported an increase in the defluoridation capacity from 0.9 to 2.8 mg/g at 48 h when F^--saturated bone char (2 g/L) was used for defluoridation of 10 mg F^-/L solution by amending 360 mg Ca^{2+}/L. Nevertheless, in the previous work, amending a high amount of Ca^{2+} to F^- water exceeds the desirable (75 mg Ca^{2+}/L) and permissible (200 mg Ca^{2+}/L) limits of Ca^{2+} in the defluoridated water.

Further defluoridation experiments conducted by amending a higher concentration of Ca^{2+} (10–40 mg Ca^{2+}/L) are presented in Table 2. These experiments show that defluoridation capacity was further enhanced from 6.21 ± 0.05 to 7.48 ± 0.02 mg/g when amended Ca^{2+} was increased from 10 to 40 mg Ca^{2+}/L at the end of 24 h. It is encouraging to note that we have observed 3.92 mg/g additional removal capacity for 40 mg Ca^{2+}/L with 24 h contact time, which is twice compared to the previous work, even we have used 9 times lower Ca^{2+} with half of the contact time used in the previous study by Jacobsen and Dahi (1997). Thus, synthetic HAP can be used efficiently for defluoridation without altering the quality of drinking water by amending 20 mg Ca^{2+}/L of aqueous calcium to 10 mg F^-/L water.

3.7. Mechanism of defluoridation using hydroxyapatite in the presence of aqueous calcium

The facts adduced above show that the likely participation of aqueous Ca^{2+} in defluoridation. Hence, defluoridation by HAP is not only just by the adsorption of F^- ion onto HAP (Sundaram et al., 2008) and F^- ion exchange with OH^- ion (Fan et al., 2003; Sundaram et al., 2008) mechanisms as reported earlier. Therefore, possible mechanisms involved in the defluoridation process when amended aqueous Ca^{2+} to F^- water are as follows:

(i) precipitation of CaF_2 in the F–Ca solution,
(ii) precipitation of F^- containing minerals such as FAP and CaF_2 when HAP dissolves,
(iii) adsorption of F^- ion or F^--complex onto the HAP surface, and
(iv) the ion exchange of F^- ion with OH^- ion into the HAP

The SIs of the solution containing both F^- (10 mg F^-/L) and Ca^{2+} (1, 3, and 5 mg Ca^{2+}/L) at pH 7 before suspending HAP were undersaturated with respect to CaF_2 mineral (Table S3); hence, CaF_2 precipitation did not occur for $Ca^{2+} \leq 5$ mg Ca^{2+}/L. Whereas, the feed solution containing 7 mg Ca^{2+}/L and 10 mg F^-/L was supersaturated with respect to CaF_2 (SI = 0.037). However, no change in the F^- concentration was observed after filtration of 24 h equilibrated CaF_2 supersaturated feed solution using 0.2 μm membrane filter. Jacobsen and Dahi (1997) also reported that the addition of a high level of Ca^{2+} (360 mg Ca^{2+}/L) to F^- water (10 mg F^-/L) did not reduce the concentration of F^- even after 48 h of contact time. Hence, it seems that a simple addition of Ca^{2+} to F^- water cannot remove F^- instantly. Therefore, it is believed that the defluoridation did not occur by the precipitation of CaF_2 mineral in the absence of HAP. Hence, the mechanism (i) will not be considered for further discussion.

Precipitation of potential minerals such as HAP, FAP, β-tricalcium phosphate ($Ca_3(PO_4)_2$), and CaF_2 could decrease the concentrations of Ca^{2+} and PO_4^{3-} ions in the defluoridated solution if it is supersaturated with respect to these potential minerals. However, defluoridated water was undersaturated with respect to all minerals considered for $F^- = 10$ mg F^-/L and $Ca^{2+} = 1$–5 mg Ca^{2+}/L (Table S3). But when 7 mg Ca^{2+}/L was amended, it was supersaturated with respect to only FAP at 1 h, and undersaturated with respect to all minerals considered for higher contact times (Table S3). Hence, possibly a defluoridation occurred by FAP precipitation between 1 and 6 h of contact time for 7 mg Ca^{2+}/L, and it is indicated by the decrease in the residual PO_4^{3-} concentration from 0.26 ± 0.02 to 0.156 ± 0.004 mg PO_4^{3-}/L (Fig. 1b). According to the MINEQL + model, 23.05 μg/L of FAP can precipitate for the sample collected at 1 h for initial $Ca^{2+} = 7$ mg Ca^{2+}/L. However, this FAP precipitation can only remove 0.87 μg F^-/L between 1 and 6 h, which is much lower than the actual F^- removed (0.98 mg F^-/L). Thus, a huge difference is observed between the actual F^- removed in the system and that calculated removal for the FAP precipitation, which suggests a possible contribution by other mechanism(s). Contrary to these results, Sternitzke et al. (2012) did not observe the decrease in the concentration of PO_4^{3-} over 28 d of the equilibrium period, even though the solution was supersaturated with respect to FAP. However, a study by the same research group reported the presence of like apatite minerals such as HAP and/or FAP onto strontium substituted HAP surface (Sternitzke et al., 2014). In the later study, authors soaked an apatite in a solution containing Ca^{2+} and PO_4^{3-} ions for 3 d in the presence and absence of F^- ion. Hence, there is a possibility of FAP precipitation onto HAP surface in the presence of solid minerals. However, further study is required to examine whether the precipitation of FAP can also occur in the absence of HAP for same ambient conditions. Thus, it is considered that the mechanism (ii) was contributed for the defluoridation at 1 h when amended 7 mg Ca^{2+}/L.

As discussed earlier, the reduction of residual Ca^{2+} and enhancement of defluoridation capacity indicated the participation of aqueous Ca^{2+} in defluoridation. The speciation of the feed solution containing F^- and Ca^{2+} ions at pH 7 shows the presence of trace concentrations of CaF^+ species. Hence, the decrease in the concentration of Ca^{2+} can be attributed either to the adsorption of only Ca^{2+} ions or its species, CaF^+ onto the HAP surface. Additional experiments conducted by suspending HAP in Ca^{2+} solution (0, 1, 5, and 20 mg Ca^{2+}/L) without F^- are presented in Fig. 3. It is clear from Fig. 3a that the dissolution of HAP occurred for $Ca^{2+} = 0$, 1 and 5 mg Ca^{2+}/L, whereas adsorption of Ca^{2+} occurred for $Ca^{2+} = 20$ mg Ca^{2+}/L. Hence, the reduction in Ca^{2+} concentration for amended 20 mg Ca^{2+}/L indicates the possibility of adsorption of aqueous Ca^{2+} from the solution. However, an increase in the pH (Fig. 3b) and the presence of PO_4^{3-} (Fig. 3c) ions in treated water showed that the HAP dissolved for all values of Ca^{2+}. Thus, adsorption of Ca^{2+} ion onto the HAP surface for $Ca^{2+} = 1$ and 5 mg Ca^{2+}/L cannot be observed clearly due to the dissolution of HAP also leaches Ca^{2+} ions to the solution. Hence, the amount of Ca^{2+} leached by HAP dissolution was calculated using the value of PO_4^{3-} concentration by assuming that the HAP dissolves with the ideal Ca/P molar ratio of 1.67. When HAP dissolution was considered, re-adsorption of Ca^{2+} ions occurred when the initial $Ca^{2+} = 5$ and 20 mg Ca^{2+}/L (Fig. 3d). However, the readsorption of Ca^{2+} did not occur for initial $Ca^{2+} = 1$ mg Ca^{2+}/L, which might be because of low concentration of Ca^{2+}. Additionally, an increase in the value of amended aqueous Ca^{2+} from 0 to 20 mg Ca^{2+}/L lowered the increase in the residual values of pH and PO_4^{3-} concentration (Fig. 3b and c). Hence, it suggests that the values of pH and PO_4^{3-} increased when Ca^{2+} was unavailable or low in the water solution. It is evident from these results that the presence of aqueous Ca^{2+} reduced the dissolution of HAP. From Figs. 1c and 3d, the reduction of aqueous Ca^{2+} (0.30 ± 0.03 mg Ca^{2+}/L) in the absence of F^- is much lower than that in the presence of F^- (4.47 ± 0.05 mg Ca^{2+}/L) at the end of 24 h of contact time when 5 mg Ca^{2+}/L aqueous calcium

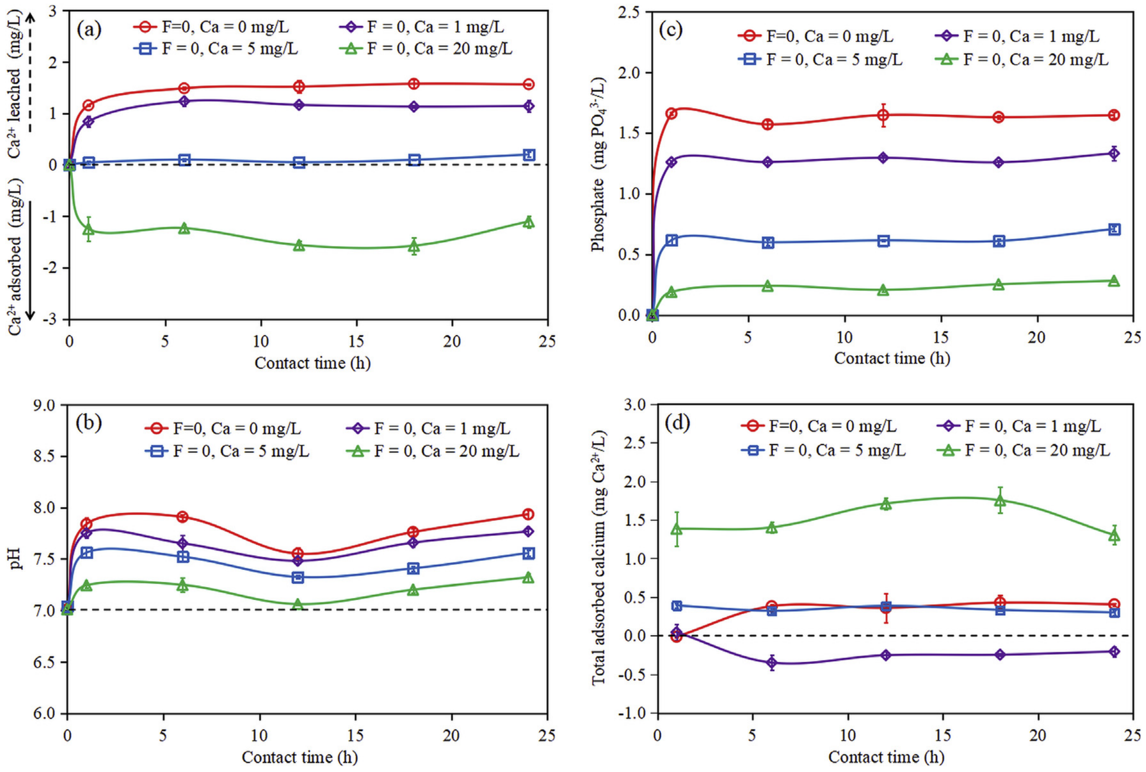

Fig. 3. The effect of amended aqueous calcium (0, 1, 5, and 20 mg Ca^{2+}/L) without fluoride on residual (a) calcium, here values of positive and negative ordinates represent Ca^{2+} leached by HAP dissolution, and that adsorbed onto the HAP, respectively, (b) pH, (c) phosphate, and (d) the total calcium adsorbed onto HAP surface when calcium leaching by HAP dissolution is considered, here positive and negative values on the ordinates represent total Ca^{2+} adsorbed and that leached from HAP, respectively. Data points and error bars represent average values of three replicates and the 95% confidence limits, respectively; sometimes error bars are smaller than symbols.

was used. Therefore, the large difference in Ca^{2+} adsorbed suggests that the defluoridation also occurred by the adsorption of CaF^{+} species onto the HAP surface. Hence, any competitive anions which form bond with Ca^{2+} can affect the formation of CaF^{+} in the solution, which further negatively impact on the defluoridation kinetics. Tang et al. (2018) reported the presence of PO_4^{3-} anion significantly reduced the defluoridation capacity of HAPs, which was due to the fact that PO_4^{3-} can easily form bond with Ca^{2+} in competition with F^{-} (Nie et al., 2012), which supports the fact that the presence any anions which form complex with Ca^{2+} can reduce the defluoridation. Bengtsson and Sjöberg (2009) and Bengtsson et al. (2009) reported the presence of ≡CaF sites on the apatite surfaces. Hence, possibly adsorption of CaF^{+} species from the solution containing F^{-} and Ca^{2+} ions formed ≡CaF sites onto the HAP surface. Thus, these results reveal the possible contribution of the adsorption of CaF^{+} complex onto the HAP surface (i.e., mechanism (iii)) for defluoridation.

Adsorption of CaF^{+} complex could reduce the Ca^{2+} and F^{-} concentrations in the molar ratio of 1:1. However, in the present study, Ca/F molar ratio for removal is always less than 1 for all values of aqueous Ca^{2+} (Fig. 4). This molar Ca/F < 1 suggests the contribution of other mechanisms, i.e., by the ion exchange (IE) and/or adsorption of CaF^{+}, which could be formed by Ca^{2+} leached from the HAP dissolution. As discussed earlier in subsection 3.4, HAP did not dissolve for $Ca^{2+} = 30$ and 40 mg Ca^{2+}/L, hence, CaF^{+} could not be formed by leached Ca^{2+}. However, the pH of the defluoridated water was increased from 7 to 7.28 ± 0.07 at 24 h even though the HAP dissolution did not occur in these experiments. Thus, the increase in the pH of defluoridated water can be attributed to the IE (mechanism (iv)), in which exchange of F^{-} with OH^{-} ion increases the pH.

The natural dissolution of HAP exposed to F^{-} solution in the absence of aqueous Ca^{2+} complicates the analysis of defluoridation by the IE. Defluoridation occurred by IE forms FAP into the F^{-} treated HAPs.

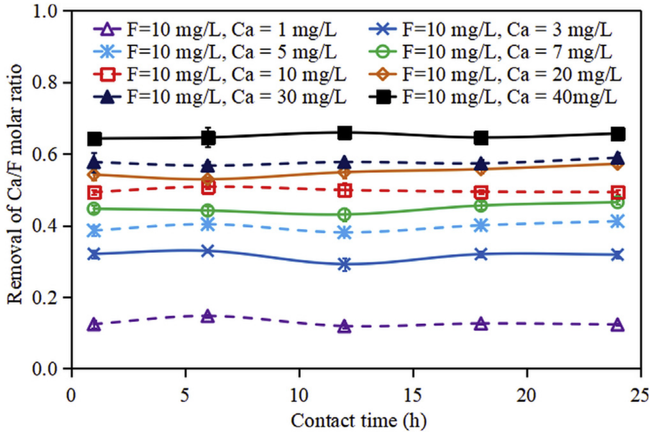

Fig. 4. Removal of Ca/F molar ratio from aqueous solution when aqueous calcium (1–40 mg Ca^{2+}/L) was amended to 10 mg F^{-}/L solution. Data points and error bars represent average values of three replicates and the 95% confidence limits, respectively; sometimes error bars are smaller than symbols.

Previous studies (Sternitzke et al., 2012; Kanno et al., 2014) reported the formation of FAP when HAP was used for defluoridation. However, in the present study, the increase in the concentration of aqueous Ca^{2+} reduces the availability of free F^{-} ions by forming Ca–F complex in the F–Ca solution. Hence, an increase in the amended aqueous Ca^{2+} concentration may affect the defluoridation by IE mechanism. The amount of FAP formed in F–Ca treated HAPs was examined using the method reported by Sternitzke et al. (2012) with the help of FTIR data.

HAP samples treated in F^{-} and F–Ca solutions were calcined at 700 °C for 3 h and used for the FTIR spectra. The substitution of the F^{-} ion by IE mechanism decreases the intensity of an OH^{-} peak at

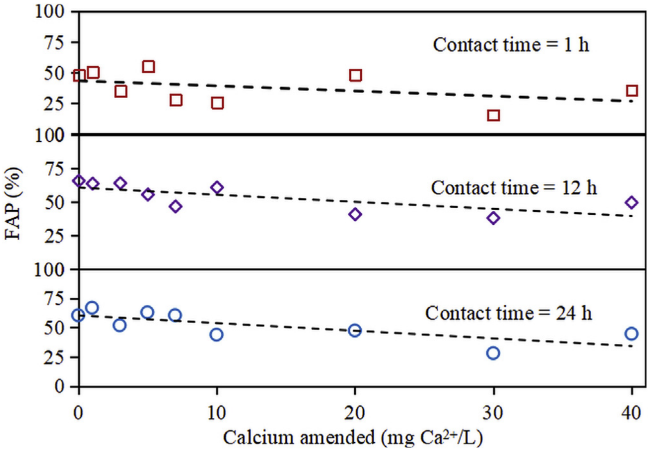

Fig. 5. Fluorapatite, FAP (%) formed when the HAP was treated in the solution containing fluoride (10 mg F^-/L) and calcium (0–40 mg Ca^{2+}/L) at (a) 1 h, (b) 12 h, and (c) 24 h contact time. Here the quantity of FAP (%) formed was measured using the FTIR spectra of HAPs.

630 cm^{-1} (Sternitzke et al., 2012). From Fig. 5, the formation of FAP declined as an increase in the initial concentration of amended Ca^{2+} from 0 to 40 mg Ca^{2+}/L for a contact time of 1, 12, and 24 h. This indicates the degree of defluoridation by IE mechanism was decreased with the increase in the concentration of amended aqueous Ca^{2+}. Hence, the reduction in the degree of IE is probably because of a decline in the availability of free F^- ions as an increase in amended Ca^{2+} forms more CaF^+ species.

In conclusion, the defluoridation was occurred by mechanisms (iii) and (iv), when aqueous Ca^{2+} was 0–5 and 20–40 mg Ca^{2+}/L, and by mechanisms (ii) to (iv) occurred when Ca^{2+} = 7 and 10 mg Ca^{2+}/L were used. The results from the present study suggest that the mechanism of defluoridation by HAP varies based on ionic composition. Further study is required to quantify the contribution of each mechanism, which is outside the scope of the present study.

4. The practical implications of the aqueous calcium amended-hydroxyapatite defluoridation method

Inexpensive and readily available raw materials such as limestone and diammonium phosphate fertilizer can be used for the synthesis of HAP media at fluorosis affected villages. However, the defluoridation using HAP without amending Ca^{2+} provides Ca^{2+}-deficient drinking water with high values of pH and residual PO_4^{3-}. Moreover, the concentration of Ca^{2+} has a negative correlation with F^- concentration in groundwater (Brindha et al., 2011; Rafique et al., 2015). Further, the defluoridation of field water using nano-HAP reduced the total hardness from 70 mg $CaCO_3$/L to zero in spite of defluoridation (Sundaram et al., 2008). Hence, drinking of this Ca^{2+}-deficit and PO_4^{3-} containing defluoridated water may pose a problem of osteoporosis as PO_4^{3-} presence consumes Ca^{2+} for precipitation of insoluble calcium phosphate. Thus, drinking of defluoridated water using HAP may pose an adverse impact on the health of individuals. The defluoridation method suggested in this study, i.e., amending aqueous Ca^{2+} to F^- water not only removes excess F^- but also provides Ca^{2+} enriched alkaline drinking water with no contamination of PO_4^{3-}. Few studies (Gupta et al., 1996; Susheela and Bhatnagar, 2002) reported the possibility of reversal of fluorosis when supplied Ca^{2+} diet to the fluorosis affected children. Notably, the presence of Ca^{2+} also reduces the bioavailability of F^- ion by forming an insoluble Ca–F complex, which decreases the absorption of F^- in the body (Cerklewski, 1997). Accumulation of F^- into the body takes place through the absorption of HF and its formation decreases with the increase in pH (Sharma et al., 2010). Hence, drinking alkaline water reduces the chances of F^- absorption into the body. Thus, amending aqueous Ca^{2+} to F^- contaminated water not just only efficiently removes F^- but may also help in reducing the risk of Ca^{2+} deficiency and F^- toxicity. Further, amending Ca^{2+} may also assist in the reversal of fluorosis and improves the life of HAP. Hence, it believes that defluoridation using "*aqueous calcium amended - hydroxyapatite*" method can be a sustainable option to provide potable drinking water to the fluorosis affected areas without compromising the quality of drinking water.

5. Conclusions

The present study suggests the defluoridation method for fluorosis affected rural areas where fluoride removal media can be synthesized in the field. The material used, i.e., hydroxyapatite and amending aqueous calcium to fluoride contaminated water can efficiently remove fluoride from drinking water. Briefly, the conclusions drawn from this study are summarized below:

Use of hydroxyapatite without amending aqueous Ca^{2+} for defluoridation provides drinking water containing PO_4^{3-} and high pH, and without Ca^{2+}. Hence, amending aqueous Ca^{2+} to F^- contaminated water successfully suppressed the dissolution of hydroxyapatite, and it also enhanced the rate of defluoridation kinetics, which is one of the key findings from the present study. The results suggested the possible contribution of adsorption of aqueous CaF^+ species onto the hydroxyapatite for defluoridation when amended aqueous Ca^{2+} to F^- water in addition to the ion exchange of F^- with OH^- ion. It is noteworthy that the defluoridation method suggested in this study, i.e., using HAP and amending aqueous Ca^{2+} to F^- water, did not add any toxic chemicals, which would affect the quality of defluoridated water. Therefore, a simple HAP preparation method and efficient defluoridation reveals its future potential application for alleviating fluorosis by providing potable Ca^{2+}-enriched and alkaline drinking water with a relatively low level of F^-.

Acknowledgements

The authors thank the Sophisticated Analytical Instruments Facility, Department of Metallurgical Engineering and Materials Science, and Central Facility-IRCC, IIT Bombay for FTIR, XRD, and HRTEM data, respectively. The authors also thank Professor Mohammed S. Razzaque, Department of Pathology, Lake Erie College of Osteopathic Medicine, Erie, PA, USA for his helpful discussion on phosphate toxicity. This research did not receive any specific grant from funding agencies in the public, commercial, or not-for-profit sectors.

Appendix A. Supplementary data

Supplementary data to this article can be found online at https://doi.org/10.1016/j.jenvman.2019.05.088.

References

Aljerf, L., Choukaife, A.E., 2017. Hydroxyapatite and fluoroapatite behavior with pH change. Int. Med. J. 24 (5), 407–410.
Anjaneyulu, L., Kumar, E.A., Sankannavar, R., Rao, K.K., 2012. Defluoridation of drinking water and rainwater harvesting using a solar still. Ind. Eng. Chem. Res. 51, 8040–8048.
Anukam, C.C., Agu, B.N., 2017. Health implications of inorganic phosphate additives in food products: a systematic review. Int. J. Community Med. Public Health 4, 1445–1449.
Ayoob, S., Gupta, A.K., Bhat, V.T., 2008. A conceptual overview on sustainable technologies for the defluoridation of drinking water. Crit. Rev. Environ. Sci. Technol. 36, 401–470.
Bahdod, A., El Asri, S., Saoiabi, A., Coradin, T., Laghzizil, A., 2009. Adsorption of phenol from an aqueous solution by selected apatite adsorbents: kinetic process and impact of the surface properties. Water Res. 43, 313–318.
Bengtsson, Å., Shchukarev, A., Persson, P., Sjöberg, S., 2009. Phase transformations, ion-exchange, adsorption, and dissolution processes in aquatic fluorapatite systems. Langmuir 25, 2355–2362.
Bengtsson, Å., Sjöberg, S., 2009. Surface complexation and proton-promoted dissolution

in aqueous apatite systems. Pure Appl. Chem. 81, 1569–1584.

Bhatnagar, A., Kumar, E., Sillanpää, M., 2011. Fluoride removal from water by adsorption - a review. Chem. Eng. J. 171, 811–840.

Brindha, K., Rajesh, R., Murugan, R., Elango, L., 2011. Fluoride contamination in groundwater in parts of Nalgonda district, Andhra Pradesh, India. Environ. Monit. Assess. 172, 481–492.

Brown, R.B., Razzaque, M.S., 2015. Dysregulation of phosphate metabolism and conditions associated with phosphate toxicity. BoneKEy Rep. 4, 705.

Bureau of Indian Standards, 2012. Indian Standard: Drinking Water Specification. Bureau of Indian Standards, New Delhi.

Cerklewski, F.L., 1997. Fluoride bioavailability-nutritional and clinical aspects. Nutr. Res. 17, 907–929.

Choukaife, A.E., Aljerf, L., 2017. A descriptive study - in vitro: new validated method for checking HAp and FAp behaviours. Int. Med. J. 24 (5), 394–397.

Delgadillo-Velasco, L., Hernández-Montoya, V., Cervantes, F.J., Montes-Morán, M.A., Lira-Berlanga, D., 2017. Bone char with antibacterial properties for fluoride removal: preparation, characterization and water treatment. J. Environ. Manag. 201, 277–285.

Fan, X., Parker, D.J., Smith, M.D., 2003. Adsorption kinetics of fluoride on low cost materials. Water Res. 37, 4929–4937.

Fawell, J., Bailey, K., Chilton, J., Dahi, E., Fewtrell, L., Magara, Y., 2006. Fluoride in Drinking-Water. World Health Organization, Cornwall.

Guéguen, L., Pointillart, A., 2000. The bioavailability of dietary calcium. J. Am. Coll. Nutr. 19, 119S–136S.

Gupta, S.K., Gupta, R.C., Seth, A.K., Gupta, A., 1996. Reversal of fluorosis in children. Pediatr. Int. 38, 513–519.

He, G.L., Cao, S.R., 1996. Assessment of fluoride removal from drinking water by calcium phosphate systems. Fluoride 29, 212–216.

Heard, K., Hill, R.E., Cairns, C.B., Dart, R.C., 2001. Calcium neutralizes fluoride bioavailability in a lethal model of fluoride poisoning. J. Toxicol. Clin. Toxicol. 39, 349–353.

Izuagie, A.A., Gitari, W.M., Gumbo, J.R., 2016. Synthesis and performance evaluation of Al/Fe oxide coated diatomaceous earth in groundwater defluoridation: towards fluorosis mitigation. J. Environ. Sci. Health A 51 (10), 810–824.

Jacobsen, P., Dahi, E., 1997. Effect of calcium addition on the defluoridation capacity of bone char. In: 2nd International Workshop on Fluorosis Prevention and Defluoridation of Water, pp. 94–99.

Jain, N., Elsayed, E.F., 2013. Dietary phosphate: what do we know about its toxicity. J. Nephrol. 26, 856–864.

Kanno, C.M., Sanders, R.L., Flynn, S.M., Lessard, G., Myneni, S.C.B., 2014. Novel apatite-based sorbent for defluoridation: synthesis and sorption characteristics of nano-micro-crystalline hydroxyapatite-coated-limestone. Environ. Sci. Technol. 48, 5798–5807.

Lessard, G., 2007. Mechanisms of Fluoride Interactions with Hydroxyapatite: Implications for Understanding and Treatment of Fluorosis. B.S. Report. Princeton University, Princetone, U.S.

MacDonald, L.H., Pathak, G., Singer, B., Jaffe, P.R., 2011. An integrated approach to address endemic fluorosis in Jharkhand, India. J. Water Resour. Prot. 3, 457–472.

Medellin-Castillo, N.A., Padilla-Ortega, E., Tovar-García, L.D., Leyva-Ramos, R., Ocampo-Pérez, R., Carrasco-Marín, F., Berber-Mendoza, M.S., 2016. Removal of fluoride from aqueous solution using acid and thermally treated bone char. Adsorption 22, 951–961.

Meenakshi, Maheshwari, R.C., 2006. Fluoride in drinking water and its removal. J. Hazard Mater. 137, 456–463.

Mohapatra, M., Anand, S., Mishra, B.K., Giles, D.E., Singh, P., 2009. Review of fluoride removal from drinking water. J. Environ. Manag. 91, 67–77.

Moshfegh, A., Goldman, J., Ahuja, J., Rhodes, D., LaComb, R., 2009. What We Eat in America, NHANES 2005–2006: Usual Nutrient Intakes from Food and Water Compared to 1997 Dietary Reference Intakes for Vitamin D, Calcium, Phosphorus, and Magnesium. U.S. Department of Agriculture, Agricultural Research Service.

Nie, Y., Hu, C., Kong, C., 2012. Enhanced fluoride adsorption using Al (III) modified calcium hydroxyapatite. J. Hazard Mater. 233–234, 194–199.

Patel, S.C., Khalkho, R., Patel, S.K., Sheikh, J.M., Behera, D., Chaudhari, S., Prabhakar, N., 2014. Fluoride contamination of groundwater in parts of Eastern India and a preliminary experimental study of fluoride adsorption by natural haematite iron ore and synthetic magnetite. Environ. Earth Sci. 72, 2033–2049.

Prasad, N., Bhadauria, D., 2013. Renal phosphate handling: Physiology. Indian J. Endocrinol. Metab. 17, 620–627.

Rafique, T., Naseem, S., Ozsvath, D., Hussain, R., Bhanger, M.I., Usmani, T.H., 2015. Geochemical controls of high fluoride groundwater in Umarkot sub-district, Thar Desert, Pakistan. Sci. Total Environ. 530, 271–278.

Razzaque, M., 2011. Phosphate toxicity: new insights into an old problem. Clin. Sci. 120, 91–97.

Ritz, E., Hahn, K., Ketteler, M., Kuhlmann, M.K., Mann, J., 2012. Phosphate additives in food - a health risk. Dtsch. Arztebl. Int. 109, 49–55.

Samrat, M.V.V.N., Rao, K.K., SenGupta, A.K., Riotte, J., Mudakavi, J.R., 2018. Defluoridation of reject water from a reverse osmosis unit and synthetic water using adsorption. J. Water Process Eng. 23, 327–337.

Sani, T., Adem, M., Fetter, G., Bosch, P., Diaz, I., 2016. Defluoridation performance comparison of nano-hydrotalcite/hydroxyapatite composite with calcined hydrotalcite and hydroxyapatite. Water, Air, Soil Pollut. 227 (3), 90.

Schecher, W.D., McAvoy, D.C., 1992. MINEQL+: a software environment for chemical equilibrium modeling. Comput. Environ. Urban Syst. 16, 65–76.

Schmoll, O., Howard, G., Chilton, J., Chorus, I., 2006. Protecting Groundwater for Health: Managing the Quality of Drinking-Water Sources. World Health Organization, Geneva.

Sharma, R., Tsuchiya, M., Skobe, Z., Tannous, B.A., Bartlett, J.D., 2010. The acid test of fluoride: how pH modulates toxicity. PLoS One 5, e10895.

Shreyas, L., Kanwar, L., Rao, K.K., 2013. Chemical engineering and the mitigation of fluorosis. Indian Chem. Eng. 55, 38–49.

Smičiklas, I., Dimović, S., Plećaš, I., Mitrić, M., 2006. Removal of Co^{2+} from aqueous solutions by hydroxyapatite. Water Res. 40, 2267–2274.

Sternitzke, V., Janousch, M., Heeb, M.B., Hering, J.G., Johnson, C.A., 2014. Strontium hydroxyapatite and strontium carbonate as templates for the precipitation of calcium-phosphates in the absence and presence of fluoride. J. Cryst. Growth 396, 71–78.

Sternitzke, V., Kaegi, R., Audinot, J.-N., Lewin, E., Hering, J.G., Johnson, C.A., 2012. Uptake of fluoride from aqueous solution on nano-sized hydroxyapatite: examination of a fluoridated surface layer. Environ. Sci. Technol. 46, 802–809.

Sundaram, C.S., Viswanathan, N., Meenakshi, S., 2008. Defluoridation chemistry of synthetic hydroxyapatite at nano scale: equilibrium and kinetic studies. J. Hazard Mater. 155, 206–215.

Susheela, A.K., 1999. Fluorosis management programme in India. Curr. Sci. 77, 1250–1256.

Susheela, A.K., 2002. Fluorosis in developing countries: remedial measures and approaches. Proc. Indian Natl. Sci. Acad. B68, 389–400.

Susheela, A.K., 2007. A Treatise on Fluorosis. Fluorosis Research and Rural Development Foundation, New Delhi, India.

Susheela, A.K., Bhatnagar, M., 2002. Reversal of fluoride induced cell injury through elimination of fluoride and consumption of diet rich in essential nutrients and antioxidants. Mol. Cell. Biochem. 234, 335–340.

Tang, Q., Duan, T., Li, P., Zhang, P., Wu, D., 2018. Enhanced defluoridation capacity from aqueous media via hydroxyapatite decorated with carbon nanotube. Front. Chem. 6, 104.

Whelton, H.P., Ketley, C.E., McSweeney, F., O'mullane, D.M., 2004. A review of fluorosis in the European Union: prevalence, risk factors and aesthetic issues. Community Dent. Oral Epidemiol 32, 9–18.

Yadugiri, V.T., 2011. Fluorosis: a persistent problem. Curr. Sci. 100 (10), 1475–1477.

Yakub, I., Soboyejo, W., 2013. Adsorption of fluoride from water using sintered clay-hydroxyapatite composites. J. Environ. Eng. 139, 995–1003.

Supplementary material for

An imperative approach for fluorosis mitigation: Amending aqueous calcium to suppress hydroxyapatite dissolution in defluoridation

Ravi Sankannavar[a,b,*], Sanjeev Chaudhari[a]

[a]*Centre for Environmental Science and Engineering, Indian Institute of Technology Bombay, Powai, Mumbai - 400 076, India*
[b]*Department of Chemical Engineering, Indian Institute of Technology Bombay, Powai, Mumbai - 400 076, India*

---

[*] Corresponding author at: Department of Chemical Engineering, Indian Institute of Technology Bombay, Powai, Mumbai - 400 076, India

Email address: `ravi.sankannavar@gmail.com` (Ravi Sankannavar)

Preprint submitted to Journal of Environmental Management *January 12, 2019*

S1. Materials and methods

S1.1. Chemicals and materials

The deionized water (EASYpure® RoDI, resistivity of 18 ΩM-cm) was used for preparation of reagents and synthetic F^- and Ca^{2+} solutions. The polyethylene bottles were used for batch experiments and storing samples. The bottles were washed with dilute hydrochloric acid (1:1) solution, followed by washing with tap water, and then rinsed thrice with deionized water. All chemicals used in this study were of at least analytical grade and used without further purification.

S1.2. Characterizations of uncalcined hydroxyapatite

The powder dried at 80 °C was characterized by the Fourier transform infrared (FTIR) spectroscopy and powder X-ray diffraction (XRD), and were used for identification of functional bands present and phase formed in the uncalcined powder, respectively. The FTIR spectra of the synthesized powder was obtained using a microscope (3000 Hyperion, Bruker). The KBr pellet method was used for FTIR and acquired the spectra over the range 4000 - 400 cm^{-1}. The powder X-ray diffraction (EMPYREAN, PANalytical) with Cu Kα (30 mA and 40 kV) used with a scanning rate of 0.017° (2θ)/20 s and for the range of 10 - 90° (2θ) to examine the formation of HAP. The size, shape, and Ca/P atomic ratio of HAPs (a) untreated (HAP), (b) treated in deionized water without F^- and Ca^{2+} (DI-HAP), (c) treated only in 10 mg F^-/L solution (F-HAP), and (d) treated in 10 mg F^-/L and 40 mg Ca^{2+}/L solution (F-Ca-HAP) for 24 h were analysed by the transmission electron microscopy (TEM). The samples for TEM analysis were prepared by suspending 1 mg of HAP samples in 1 mL of ethanol and sonicated for around 2 min. The suspension of this HAP was drop-casted onto a copper TEM grids and dried under IR-lamp for 5 min. The imaging and energy dispersive spectroscopy (EDS) of HAP samples were carried out in a JEOL 2100 HRTEM equipped with INCAx-Sight EDS detector (Oxford Instruments), which was operated at 200 kV at room temperature (23 °C).

S1.3. Measurement of Ca/P molar ratio and the specific surface area

The actual Ca/P molar ratio of HAP was measured by dissolving 20 mg HAP in 1 mL of 35 % HCl solution. This HAP solution was diluted to 100 mL with deionized water and measured the concentrations of Ca^{2+} and PO_4^{3-} ions. The specific surface areas were measured by a single point Brunauer-Emmet-Teller (BET) theory using a Micrometrics ASAP-2020 (V3.00 H) surface area analyser at 77.6 K. First, samples (0.31 g) were de-gasified at room temperature (25 °C) for 500 min and then used for analysis. The effect of calcination on the surface area of HAP was examined by measuring the BET surface area of HAPs dried at 80 °C (uncalcined) and heat-treated at 700 °C for 3 h (calcined). However, only uncalcined HAP was used for defluoridation experiments.

S1.4. Aqueous solution analysis

Aqueous solutions were analysed before and after experiments by measuring the pH and concentrations of F^-, Ca^{2+}, and PO_4^{3-} ions. Immediately after filtration, the pH of treated water was measured using a glass combination pH electrode (Orion 8102BNUWP, Thermo Scientific) coupled with a pH benchtop meter (Orion 3 Star, Thermo Scientific). The F^- concentration was measured using a F^- ion selective electrode (Orion 9609BNWP, Thermo Scientific) coupled with a pH/ISE benchtop meter (Orion Star A214, Thermo Scientific). This ISE meter was calibrated using F^- standards (0.1, 1, and 10 mg F^-/L) containing 50 % of TISAB II (Orion 940909, Thermo Scientific) by volume. Hence, TISAB II was added to the samples to be analysed. The PO_4^{3-} and

Ca^{2+} concentrations were measured using the stannous chloride method (4500-P D) and EDTA titrimetric method (3500-Ca B) of Eaton et al. (2005), respectively.

S1.5. Calculation of saturation indices using MINEQL+

The propensity of any solids could be precipitated and chemical speciation were carried out using the MINEQL+ (Version 4.5) chemical equilibrium modeling system (Schecher and McAvoy, 1992) for each experiment conducted. The saturation indices (SIs) of solids were calculated using the equation, SI = log (IAP/K_{sp}), where IAP and K_{sp} are the ion activity product and the solubility product, respectively for solid considered. Solubility products of solids considered are $10^{-44.33}$, $10^{-28.92}$, $10^{-10.50}$, and $10^{-56.12}$ for hydroxyapatite ($Ca_5(PO_4)_3OH$), β-tricalcium phosphate ($Ca_3(PO_4)_2$ or β-TCP), fluorite (CaF_2), and fluorapatite ($Ca_5(PO_4)_3F$ or FAP), respectively. Total dissolved concentrations of Ca^{2+}, PO_4^{3-} and F^- ions, final pH, and ionic strength were used during the calculations. Values of $SI > 0$ indicate supersaturation, $SI < 0$ indicate undersaturated, and $SI = 0$ indicate equilibrium with respect to a solid considered.

S2. Results and discussion

S2.1. Characterization of synthesized uncalcined hydroxyapatite

The FTIR spectrum of synthesized uncalcined HAP is presented in Fig. S1(a). The functional groups present in the FTIR are in good agreement with FTIR data reported in the literature (Kumar et al., 2004) and the functional groups present in the sample are shown in Fig. S1(a). However, O-H liberation mode at around 630 cm^{-1} is not present. The absence of a peak at 630 cm^{-1} was due to a lower degree of HAP crystallinity, and this peak is sensitive to the heating temperature

(Berzina-Cimdina and Borodajenko, 2012). Thus, HAPs treated at high temperature (Kumar et al., 2004) and commercial HAPs (Sternitzke et al., 2012) have this O-H liberation mode.

The XRD pattern of synthesized powder in the present study is shown in Fig. S1(b) along with a reference pattern. The crystalline peaks at 2θ = 26.02, 31.98, 32.34, 33.25, 34.30, and 49.63° were compared and agreed with those of synthetic HAP (ICDD card 01-086-0740) with no trace minerals. Thus, the presence of HAP phase from XRD, and PO_4^{3-} and O-H groups from FTIR confirm that the uncalcined synthesized powder in this study was HAP.

The shape of HAPs are presented in Fig. S2 and found to be rod-like shape. The sizes of HAP particles were measured using ImageJ software and typically considered 120 - 150 particles. The Ca/P atomic ratios of HAPs were also measured using EDS, and are presented in Table S1 along with the particle size analysis.

Table S1: The Ca/P atomic ratio of HAPs (a) untreated (HAP), (b) treated in deionized water without F^- and Ca^{2+} ions (DI-HAP), (c) treated in only F^- solution (F-HAP), and (d) treated in F-Ca solution (F-Ca-HAP), which were measured using EDS and the particle size analysis was done using HRTEM. Here mean and S.D. represent the mean of 120 - 150 particles and standard deviation, respectively.

HAP	Ca/P atomic ratio	Particle size (nm)		
		Mean	S.D.	range
(a) HAP	1.57	80	15	52 - 119
(b) DI-HAP	1.52	71	17	37 - 108
(c) F-HAP	1.59	59	14	32 - 102
(d) F-Ca-HAP	1.67	78	17	41 - 121

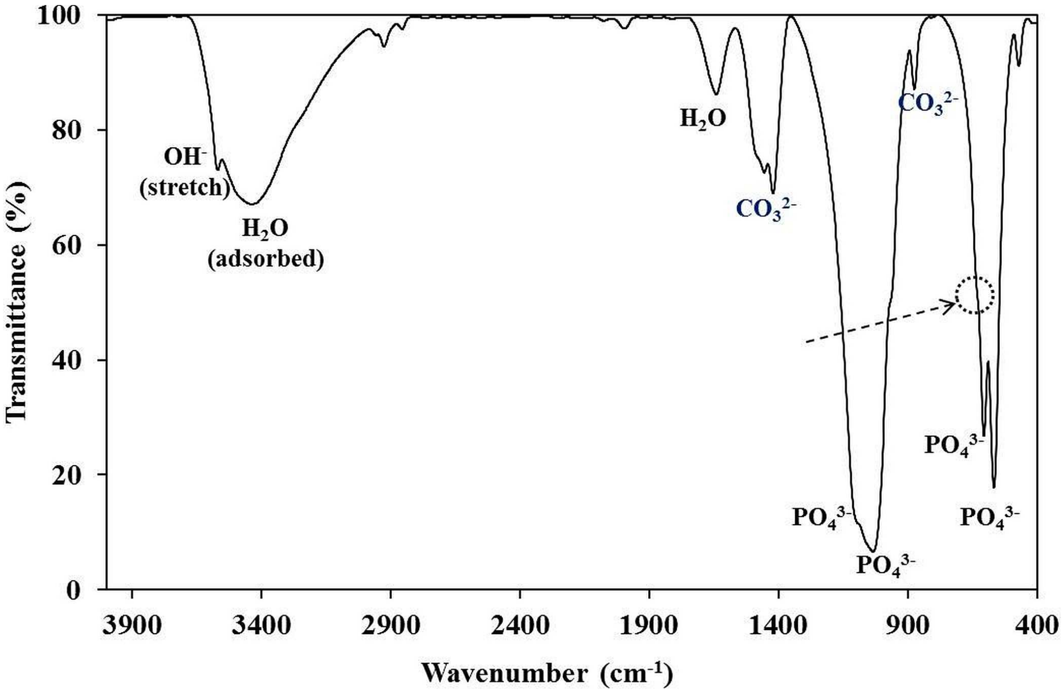

(a) FTIR

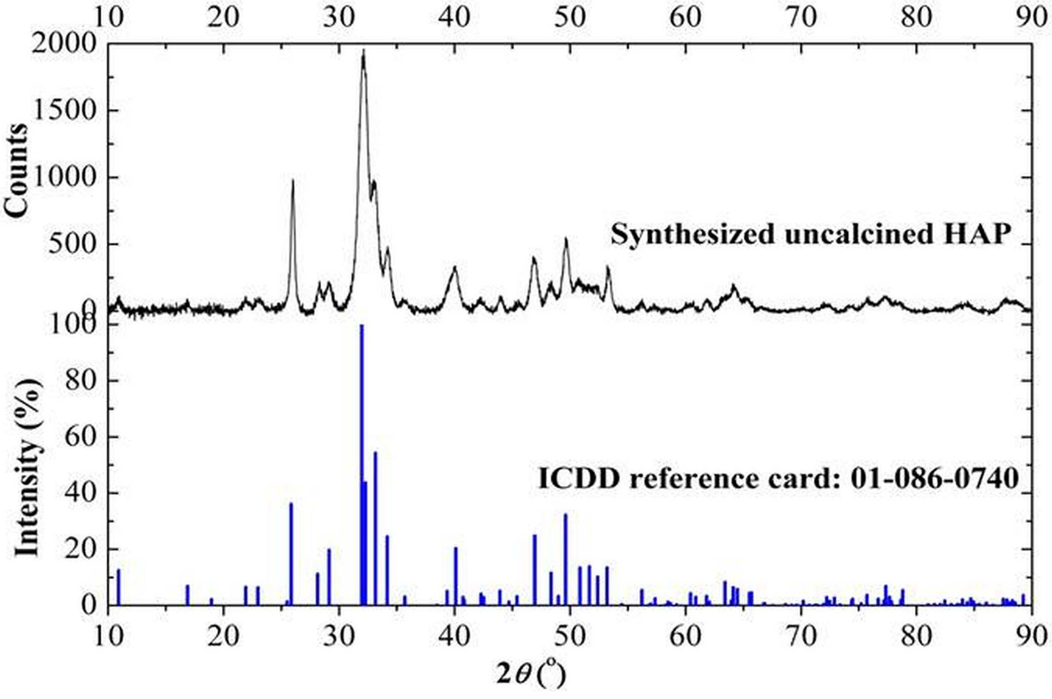

(b) XRD

Fig. S1. (a) Fourier transform infrared spectroscopy and (b) X-ray diffraction pattern of uncalcined hydroxyapatite with the ICDD reference card 01-086-0740.

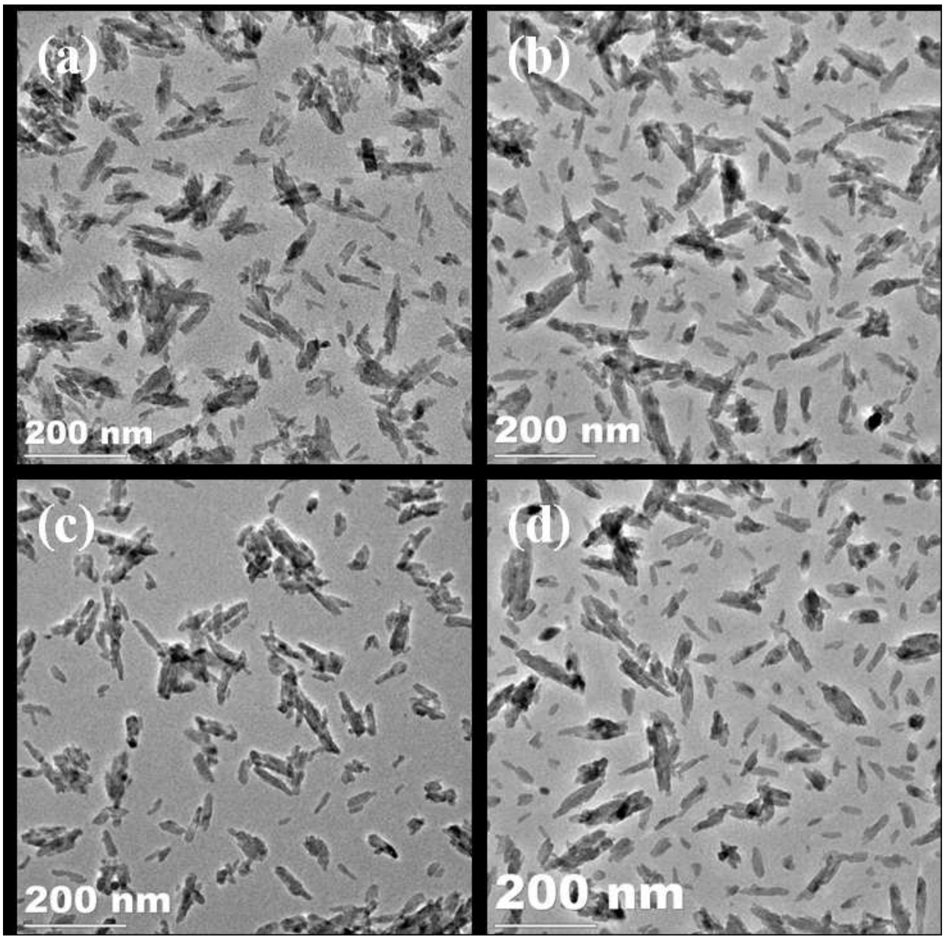

Fig. S2. HRTEM images of hydroxyapatites (a) untreated, (b) treated in deionized water without F^- and Ca^{2+} ions, (c) treated in only F^- solution, and (d) treated in F-Ca solution.

Table S2: Saturation indices for experiments conducted by suspending HAP in a solution with 10 mg F^-/L and without fluoride (F^-). Here HAP, β-TCP, FAP, and CaF_2 represent hydroxyapatite, β-tricalcium phosphate, fluorapatite, and fluorite, respectively.

	Saturation index				
Time (h)	1	6	12	18	24
Mineral	F^- = 0 mg F^-/L				
HAP	1.0 ± 0.2	2.0 ± 0.4	1.6 ± 0.1	2.2 ± 0.2	2.2 ± 0.2
β-TCP	- 3.8 ± 0.1	- 3.2 ± 0.2	- 3.39 ± 0.05	- 3.09 ± 0.08	- 3.07 ± 0.09
	F^- = 10 mg F^-/L				
HAP	- 2.2 ± 0.8	- 2.3 ± 0.8	- 2.5 ± 0.4	- 1.9 ± 0.9	- 0.4 ± 0.7
β-TCP	- 5.9 ± 0.5	- 5.9 ± 0.4	- 5.9 ± 0.5	- 5.7 ± 0.5	- 5.0 ± 0.3
FAP	- 2.2 ± 0.8	- 2.4 ± 0.6	- 2.6 ± 0.3	- 2.2 ± 0.7	- 1.0 ± 0.5
CaF_2	- 2.1 ± 0.2	- 2.38 ± 0.01	- 2.43 ± 0.01	- 2.44 ± 0.01	- 2.47 ± 0.01

Table S3: The saturation indices of defluoridation experiments conducted by amending low aqueous calcium (1 - 7 mg Ca^{2}/L) to 10 mg F^{-}/L solution. Here HAP, β-TCP, FAP, and CaF$_2$ represent hydroxyapatite, β-tricalcium phosphate, fluorapatite, and fluorite, respectively.

	Saturation index				
Time (h)	1	6	12	18	24
Mineral	Ca^{2+} = 1 mg Ca^{2+}/L				
HAP	- 0.6 ± 0.6	- 5 ± 2	- 3 ± 1	- 4 ± 2	- 2.0 ± 0.5
β-TCP	- 4.8 ± 0.3	- 7.2 ± 0.9	- 6.3 ± 0.7	- 7 ± 1	- 5.9 ± 0.2
FAP	- 0.4 ± 0.5	- 4 ± 1	- 3 ± 1	- 4 ± 2	- 2.4 ± 0.4
CaF_2	- 1.60 ± 0.09	- 2.40 ± 0.01	- 2.2 ± 0.2	- 2.47 ± 0.01	- 2.49 ± 0.01
	Ca^{2+} = 3 mg Ca^{2+}/L				
HAP	- 0.5 ± 0.3	- 3.4 ± 0.9	- 2.3 ± 0.9	- 5 ± 2	- 4.0 ± 0.5
β-TCP	- 4.7 ± 0.1	- 6.4 ± 0.5	- 5.8 ± 0.5	- 7.3 ± 0.9	- 7.0 ± 0.3
FAP	- 0.01 ± 0.2	- 2.7 ± 0.7	- 1.8 ± 0.8	- 4 ± 1	- 4.1 ± 0.5
CaF_2	- 1.16 ± 0.03	- 1.61 ± 0.03	- 1.63 ± 0.08	- 2.2 ± 0.2	- 2.49 ± 0.07
	Ca^{2+} = 5 mg Ca^{2+}/L				
HAP	- 0.7 ± 0.2	- 2 ± 1	- 2.2 ± 0.6	- 3.6 ± 0.1	- 3.0 ± 0.8
β-TCP	- 4.81 ± 0.09	- 5.8 ± 0.7	- 5.9 ± 0.7	- 6.61 ± 0.06	- 6.4 ± 0.5
FAP	- 0.1 ± 0.1	- 2 ± 1	- 1.6 ± 0.5	- 3.00 ± 0.02	- 2.7 ± 0.7
CaF_2	- 0.87 ± 0.01	- 1.20 ± 0.02	- 1.4 ± 0.1	- 1.56 ± 0.02	- 1.73 ± 0.04
	Ca^{2+} = 7 mg Ca^{2+}/L				
HAP	- 0.2 ± 0.8	- 3 ± 1	- 3.1 ± 0.3	- 3.7 ± 0.5	- 2.6 ± 0.6
β-TCP	- 4.82 ± 0.06	- 6.1 ± 0.6	- 6.4 ± 0.2	- 6.7 ± 0.3	- 6.2 ± 0.3
FAP	0.11 ± 0.09	- 2.0 ± 0.9	- 2.4 ± 0.3	- 3.0 ± 0.5	- 2.2 ± 0.5
CaF_2	- 0.69 ± 0.01	- 0.97 ± 0.03	- 1.12 ± 0.01	- 1.26 ± 0.05	- 1.36 ± 0.03

References

Berzina-Cimdina, L., Borodajenko, N., 2012. Research of calcium phosphates using Fourier transform infrared spectroscopy, in: Theophanides, T.M. (Ed.), Infrared Spectroscopy - Materials Science, Engineering and Technology. InTech, Rijeka Croatia, pp. 123–149.

Eaton, A.D., Greenberg, A.E., Clesceri, L.S., Rice, E.W., Franson, M.A.H., 2005. Standard Methods for the Examination of Water & Wastewater. 21 ed., American Public Health Association, American Water Works Association, and Water Environment Federation, New York.

Kumar, R., Prakash, K., Cheang, P., Khor, K., 2004. Temperature driven morphological changes of chemically precipitated hydroxyapatite nanoparticles. Langmuir 20, 5196–5200.

Schecher, W.D., McAvoy, D.C., 1992. MINEQL+: A software environment for chemical equilibrium modeling. Comput. Environ. Urban Syst. 16, 65–76.

Sternitzke, V., Kaegi, R., Audinot, J.N., Lewin, E., Hering, J.G., Johnson, C.A., 2012. Uptake of fluoride from aqueous solution on nano-sized hydroxyapatite: Examination of a fluoridated surface layer. Environ. Sci. Technol. 46, 802–809.